The crystal structure and magnetic properties of $R_2Fe_{17}C_x$ (x=1.5 and 2.0) prepared by the melt-spinning method

1993 J. Phys.: Condens. Matter 5 2001

(http://iopscience.iop.org/0953-8984/5/13/015)

J. Phys.: Condens. Matter 5 (1993) 2001–2008. Printed in the UK

The crystal structure and magnetic properties of $R_2Fe_{17}C_x$ ($x = 1.5$ and 2.0) prepared by the melt-spinning method

Lei Cao, Lin-shu Kong and Bao-gen Shen

State Key Laboratory of Magnetism, Institute of Physics, Chinese Academy of Sciences, PO Box 603, Beijing 100080, People's Republic of China

Received 10 August 1992, in final form 30 November 1992

Abstract. We have successfully prepared the carbides $R_2Fe_{17}C_x$ (R ≡ Y, Gd, Tb, Dy, Ho and Er) with a high carbon content $x = 1.5$ and 2.0 by the melt-spinning method. The carbides have a single rhombohedral Th_2Zn_{17} structure phase and are highly stable to at least 1100 °C. The Curie temperatures T_C are raised enormously and the saturation magnetizations change little upon carbonation. The average enhancements of T_C are about 220 K for $R_2Fe_{17}C_{1.5}$ and 265 K for $R_2Fe_{17}C_{2.0}$. The volume dependence of the exchange interaction has been discussed. The Curie temperatures are analysed in terms of a mean-field model. The spin reorientation is observed to be 133 K for $Er_2Fe_{17}C_{1.5}$ and 141 K for $Er_2Fe_{17}C_{2.0}$.

1. Introduction

Introducing interstitial atoms, such as hydrogen [1], carbon [2] and nitrogen [3–6], into R_2Fe_{17} intermetallic compounds, has improved the magnetic properties of these compounds considerably. The gas-phase nitrides $R_2Fe_{17}N_x$ ($x \simeq 2.6$) have unit-cell volumes about 6–7% larger and Curie temperatures about 400 °C higher than those of the 2:17 parent compounds [4], and $Sm_2Fe_{17}N_x$ exhibits strong uniaxial anisotropy, with a room-temperature anisotropy field of 140 kOe [7]. Early in 1988, in a study of $R_2Fe_{14}C$ compounds, a high-temperature stable interstitial carbide phase of $R_2Fe_{17}C_x$ was found [8]. Further efforts to prepare high-carbon interstitial compounds by arc melting the elements with Fe_3C led to an occupancy well below $x = 2$ [9], being limited to $x \simeq 1$ for the light rare earths, and to $x \simeq 1.5$ for the heavy rare earths. A structure change from hexagonal (Th_2Ni_{17} type) to rhombohedral (Th_2Zn_{17} type) was observed in some cases as x increased [10, 11]. The unit-cell volume expansion is about 3%, the Curie temperature T_C enhancement is about 200 °C [2] and samarium carbide has an anisotropy field of 53 kOe at room temperature [12]. Neutron diffraction showed that both nitrogen and carbon atoms occupied the octahedral interstices [6, 13, 14]. Figure 1 is the schematic representation of the rhombohedral crystal structure with the formula composition $R_2Fe_{17}C_3$, although preliminary investigations showed that the actual maximum C content in $R_2Fe_{17}C_x$ is much smaller. Recently, through the reaction of R_2Fe_{17} with gaseous hydrocarbons [15, 16], a drastic enhancement of T_C is realized in the $R_2Fe_{17}C_2$ series. A T_C of 680 K was found and an anisotropy field greater than 100 kOe was estimated for $Sm_2Fe_{17}C_2$. Microcrystalline $Sm_2Fe_{17}C_2$ powders exhibit a room-temperature coercivity of up to

0953-8984/93/132001+08$07.50

18.5 kA cm^{-1} (23.2 kOe) and a maximum energy product of 59 kJ m^{-3} (7.4 MG Oe) [17]. Both $Sm_2Fe_{17}N_x$ and $Sm_2Fe_{17}C_x$, prepared by melting and the solid–gas reaction, have striking magnetic properties, but they are unstable and decompose into the equilibrium phases RC and α-Fe upon heating to 600–700 °C in vacuum. In order to test the potential of the non-equilibrium processing in obtaining the $R_2Fe_{17}C_x$ phase, we have systematically studied the melt-spun $R_2Fe_{17}C_x$ (x = 0–3.0) series and successfully obtained high-carbon $R_2Fe_{17}C_x$ compounds. Since it is possible to prepare compounds of the compositions $R_2Fe_{17}C_{1.5}$ and $R_2Fe_{17}C_{2.0}$ in all heavy-rare-earth cases, here we have restricted our studies to the $R_2Fe_{17}C_{1.5}$ and $R_2Fe_{17}C_{2.0}$ series (R ≡ Y, Gd, Tb, Dy, Ho and Er) prepared by the melt-spinning method.

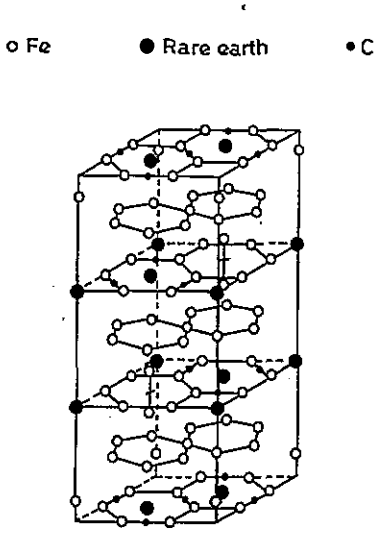

Figure 1. Schematic representation of the rhombohedral crystal structure with the formula composition $R_2Fe_{17}C_3$ (partially occupied Th_2Zn_{17} type): O, Fe; ●, rare earth; •, C.

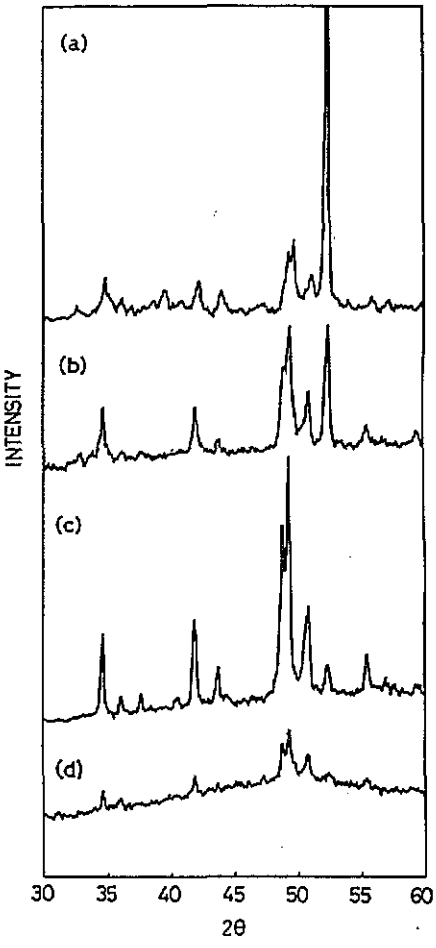

Figure 2. X-ray diffraction patterns of the $Gd_2Fe_{17}C_{2.0}$ compounds prepared by different quenching rates V_s: (*a*) 0 m s^{-1}; (*b*) 12 m s^{-1}; (*c*) 20 m s^{-1}; (*d*) 30 m s^{-1}.

2. Experiments and results

Iron rods and carbon pellets were first arc melted into Fe–C alloys, and then Fe, Fe–C and rare-earth pellets were arc melted according to the composition $R_2Fe_{17}C_x$ ($x = 1.5$, 2.0). The purities of the elements used were 99.9%. The meltings were carried out under a highly purified argon atmosphere and repeated several times to ensure homogeneity. The masses of the ingots were 25–30 g each.

For comparison, we treated the ingots in two ways: the first was by annealing the ingots at 1100 °C for 14 h under 2×10^{-5} Torr and quenching them to avoid the phase transition to $R_2Fe_{14}C$; the second was by melt spinning the ingots, followed by heat treating at 1100 °C for 14 h under 2×10^{-5} Torr. The melt-spinning process is as follows: 2–3 g ingots were induced molten and then ejected by argon air through a nozzle at the bottom of a quartz tube onto the surface of a rotating copper wheel. The surface velocity V_s of the copper wheel ranges from 0 to 47 m s^{-1}. The melt-spun ribbons are about 1–1.5 mm wide and 20–30 μm thick.

X-ray diffraction with Co Kα radiation showed that the $R_2Fe_{17}C_{1.5}$ and $R_2Fe_{17}C_{2.0}$ ingots were multiphases with RC, the 2:17 phase and a predominant α-Fe phase. The phase components of the ingots do not change when a heat treatment at 1100 °C for 14 h is applied but an enormous increase in α-Fe phase results. Melt spinning $R_2Fe_{17}C_x$ with an optimal quenching rate revealed a single phase having the rhombohedral Th_2Zn_{17} structure type. The formation of the single-phase $R_2Fe_{17}C_x$ is sensitive to the quenching rate V_s; a low V_s resulted in a high proportion of α-Fe phase, and a high V_s resulted in the formation of some amorphous phases. For different rare earths, the optimal quenching rates were different, but they were restricted in the relatively narrow range 10–20 m s^{-1}. Figure 2 illustrates the phase change versus the quenching rate V_s. Figure 3 is the x-ray diffraction diagram of the melt-spun ribbons of $Dy_2Fe_{17}C_{2.0}$ after heat treatment at 1100 °C for 14 h; the ribbons still maintain the rhombohedral Th_2Zn_{17} structure. The lattice constants a and c, the unit-cell volume V and the relative change $\Delta V/V$ in the unit-cell volume of the $R_2Fe_{17}C_{1.5}$ and $R_2Fe_{17}C_{2.0}$ series are listed in table 1.

The temperature dependence of the magnetization $\sigma(T)$ was measured in a field of 2 kOe using an automated vibrating-sample magnetometer on the optimally quenched samples, showing that the samples are almost single phase (figure 4). The values of the Curie temperature T_C determined by extrapolating the $\sigma(T)$ curves are included in table 1 and plotted as a function of the rare-earth components in figure 5. The average increase in T_C is about 220 K for $R_2Fe_{17}C_{1.5}$ and 265 K for $R_2Fe_{17}C_{2.0}$, and there is the usual dependence on the R component with a maximum for Gd.

The magnetizations are measured in a field ranging from 0 to 70 kOe at $T = 1.5$ K and $T = 300$ K. The saturation magnetizations σ_s have been included in table 1. The spin reorientation temperature T_{sr} of $Er_2Fe_{17}C_{1.5}$ and $Er_2Fe_{17}C_{2.0}$ are measured in a field of 1 kOe (figure 6).

3. Discussion

The $R_2Fe_{17}C_{1.5}$ and $R_2Fe_{17}C_{2.0}$ compounds with the heavy rare earths Y, Gd, Tb, Dy, Ho and Er have a single rhombohedral Th_2Zn_{17} crystal structure. In table 1 we have compared our results with the data for the parent R_2Fe_{17} compounds [5, 15]. The relationships between the hexagonal and rhombohedral structure are $a_h \simeq a_{rh}$

Table 1. Lattice parameters a and c, unit-cell volumes V, relative changes $\Delta V/V$ in the unit-cell volume, Curie temperatures T_C and saturation magnetizations σ_s at $T = 1.5$ K.

Compound	a (Å)	c (Å)	V (Å^3)	$\Delta V/V$ (%)	T_C (K)	M_s (μ_B/formula unit)	M_{Fe} (μ_B/formula unit)
Gd_2Fe_{17}[a]	8.537	12.424	784.1				
$Gd_2Fe_{17}C_{1.5}$	8.671	12.508	814.4	3.9	647	22.1	36.1
$Gd_2Fe_{17}C_{2.0}$	8.681	12.533	817.9	4.3	675	22.9	36.9
Tb_2Fe_{17}[a]	8.473	8.323	517.5				
$Tb_2Fe_{17}C_{1.5}$	8.643	12.465	806.4	3.9	610	16.4	34.4
$Tb_2Fe_{17}C_{2.0}$	8.664	12.536	814.9	5.0	656	17.4	35.4
Dy_2Fe_{17}[a]	8.767	8.312	516				
$Dy_2Fe_{17}C_{1.5}$	8.621	12.499	804.6	4.0	578	15.4	35.4
$Dy_2Fe_{17}C_{2.0}$	8.645	12.585	814.6	5.2	626	16.1	36.1
Ho_2Fe_{17}[a]	8.460	8.277	513				
$Ho_2Fe_{17}C_{1.5}$	8.601	12.500	800.9	4.1	575	16.7	36.7
$Ho_2Fe_{17}C_{2.0}$	8.633	12.529	808.6	5.1	621	16.6	36.6
Er_2Fe_{17}[a]	8.440	8.272	510.3				
$Er_2Fe_{17}C_{1.5}$	8.581	12.496	796.8	4.1	560	18.4	36.4
$Er_2Fe_{17}C_{2.0}$	8.619	12.519	805.4	5.2	610	18.1	36.1
Y_2Fe_{17}[b]	8.48	8.26	514		325		
$Y_2Fe_{17}C_{1.5}$	8.643	12.443	805.0	4.4	591	34.6	34.6
$Y_2Fe_{17}C_{2.0}$	8.664	12.492	812.0	5.3	620	36.1	36.1

[a] Values obtained from [5].
[b] Values obtained from [15].

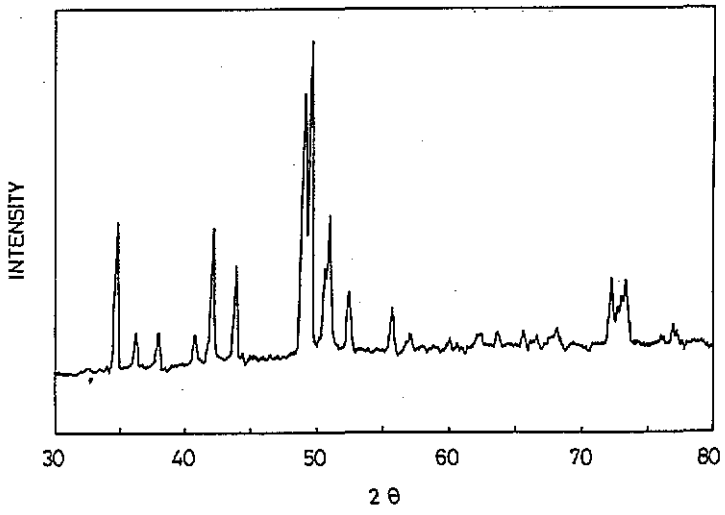

Figure 3. X-ray diffraction diagram of $Dy_2Fe_{17}C_{2.0}$ quenched at 20 m s^{-1} and annealed at 1100 °C for 14 h.

and $c_h \simeq \frac{2}{3}c_{rh}$, and we define $V_{rh} = \frac{1}{3}\sqrt{3}a_{rh}^2 c_{rh}$ and $V_h = \frac{1}{2}\sqrt{3}a_h^2 c_h$ for normalization and comparison. The unit-cell volumes follow the lanthanide constriction in the $R_2Fe_{17}C_{1.5}$ and $R_2Fe_{17}C_{2.0}$ series. The lattice parameters a and c and the unit-cell volumes V increase continuously with increasing carbon content. The melt-

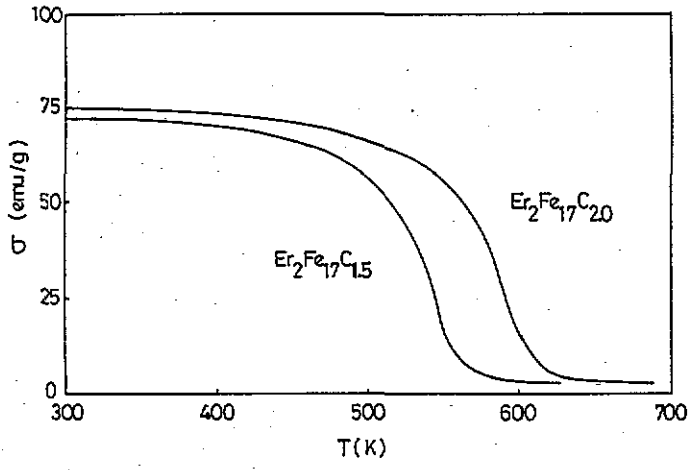

Figure 4. The temperature dependence of the magnetization $\sigma(T)$ curves of $Er_2Fe_{17}C_{1.5}$ and $Er_2Fe_{17}C_{2.0}$ compounds measured in a field of 2 kOe at room temperature.

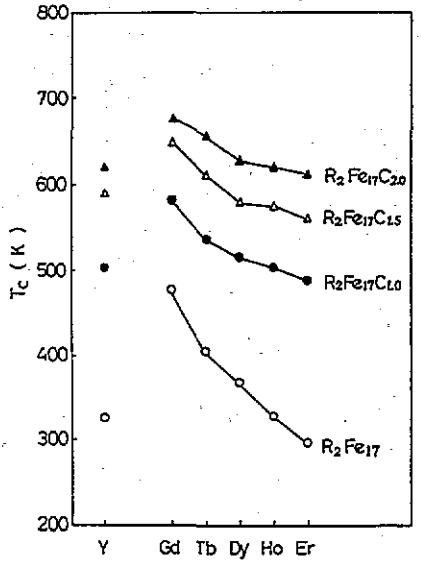

Figure 5. The Curie temperatures of R_2Fe_{17}, $R_2Fe_{17}C_{1.0}$, $R_2Fe_{17}C_{1.5}$ and $R_2Fe_{17}C_{2.0}$.

spun $R_2Fe_{17}C_{1.5}$ and $R_2Fe_{17}C_{2.0}$ compounds are rhombohedral, consistent with the melt compounds, which become rhombohedral when $x > 1$ [10, 11]; however, the $Y_2Fe_{17}C_x$ ($x \geqslant 2$) compound produced by the solid–gas reaction is hexagonal [15, 16]. The relative changes in the unit-cell volume of $R_2Fe_{17}C_{2.0}$ are comparable for these two groups. Figure 3 shows that the $R_2Fe_{17}C_{2.0}$ series prepared by melt spinning is highly stable, being quite different from the metastable carbides obtained using hydrocarbon or methane gases. As we know, the carbon atoms in the 2:17 structure have iron atoms as well as rare-earth atoms as neighbours, and the enthalpy of the R–C bond is strongly negative, contributing much to the stability of these ternary carbides [18].

The crystalline grains in the melt-spun ribbons are very small and cannot be easily

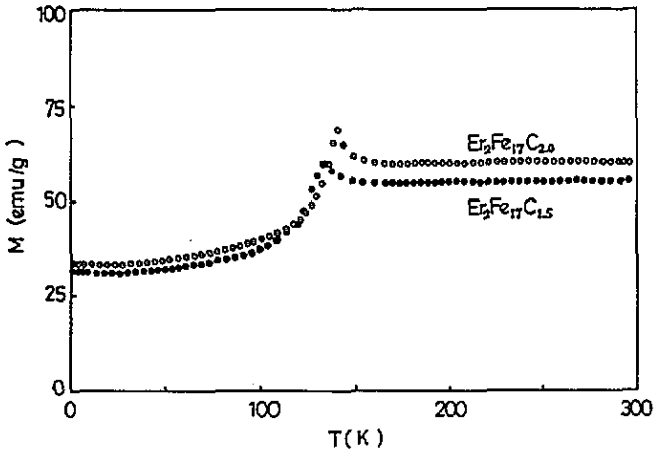

Figure 6. Temperature dependence of the magnetization $\sigma(T)$ of $Er_2Fe_{17}C_{1.5}$ and $Er_2Fe_{17}C_{2.0}$ compounds measured at $H = 1$ kOe.

magnetically aligned. After heat treatment at 1100 °C for 14 h, the grains grow larger and can be oriented in an applied field of 10 kOe.

The temperature dependence of the magnetization $\sigma(T)$ curves show that $R_2Fe_{17}C_{1.5}$ and $R_2Fe_{17}C_{2.0}$ are of single phase (figure 4). Their Curie temperatures are shown in figure 5, compared with those of the pure R_2Fe_{17} [4] and $R_2Fe_{17}C$ [2] compounds. A considerable enhancement of T_C can be observed when x increases from 0 to 2.0. For small x-values, the Curie temperatures increase with increasing carbon concentration more drastically than for larger x-values. However, there is a linear behaviour when T_C is plotted versus the corresponding unit-cell volumes. As examples, figure 7 illustrates this relationship for $R_2Fe_{17}C_x$ ($x = 0$–2.0; R ≡ Y, Gd), including the values for $Y_2Fe_{17}N_{2.6}$ [4] and $Gd_2Fe_{17}N_{2.5}$ [5] for comparison. It demonstrates the volume dependence of the exchange interaction in the 2:17 structure, and it is common for individual interstitials with different chemical features.

In the molecular-field model, the Curie temperature in the rare-earth iron series can be expressed as

$$3kT_C = a_{FeFe} + (a_{FeFe}^2 + 4a_{FeR}a_{RFe})^{1/2} \tag{1}$$

where the R–R interaction is neglected. The corresponding coupling constants J_{RFe} and J_{FeFe} can be written as follows:

$$a_{FeFe} = Z_{FeFe}J_{FeFe}S_{Fe}(S_{Fe} + 1) \tag{2}$$

$$a_{RFe}a_{FeR} = Z_{RFe}Z_{FeR}S_{Fe}(S_{Fe} + 1)(g_J - 1)^2J(J + 1)J_{RFe}^2 \tag{3}$$

where Z_{RFe}, Z_{FeR} and Z_{FeFe} are the coordination numbers in the unit cell considered. Rewriting equations (1)–(3) leads to [19]

$$J_{FeFe} = 3kT_{C,0}/2Z_{FeFe}S_{Fe}(S_{Fe} + 1) \tag{4}$$

$$J_{RFe}^2 = 9k^2(T_{C,R} - T_{C,0})T_{C,R}/4Z_{RFe}Z_{FeR}S_{Fe}(S_{Fe} + 1)(g_J - 1)^2J(J + 1). \tag{5}$$

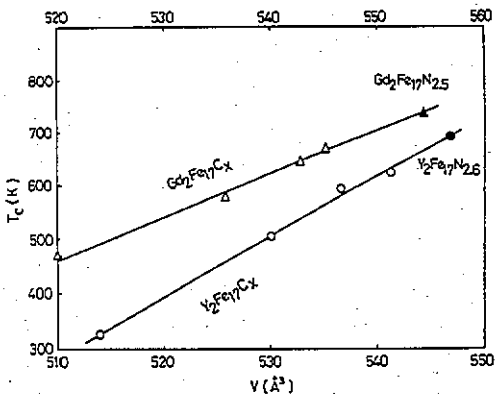

Figure 7. The unit-cell volume dependence of the Curie temperature for $R_2Fe_{17}C_x$, compared with $R_2Fe_{17}N_{2.5}$.

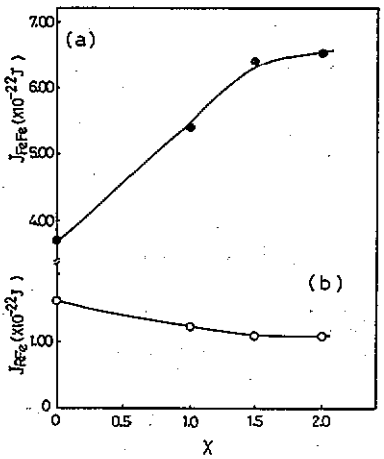

Figure 8. (*a*) The Fe–Fe exchange interaction J_{FeFe} and (*b*) the R–Fe exchange interaction J_{RFe} as functions of the carbon concentration x.

For the Th_2Ni_{17} or Th_2Zn_{17} structure, inserting $Z_{FeFe} = 9$, $Z_{RFe} = 19$, $Z_{FeR} = 2$ together with $T_{C,R}$ for Gd and $T_{C,0}$ for Y, we can obtain J_{FeFe} and J_{RFe} for the carbides $R_2Fe_{17}C_x$ with different x-values. The carbon concentration dependences of J_{FeFe} and J_{RFe} are plotted in figures 8(*a*) and 8(*b*), respectively. J_{FeFe} is approximately four to six times J_{RFe}, and it increases monotonically with increasing x, but J_{RFe} decreases slightly as the carbon concentration x increases. This indicates that the drastic enhancement of T_C is attributed to the increase in the Fe–Fe exchange interaction due to the interstitial carbon atoms. Two possible explanations for the variation in J_{RFe} across the lanthanide series were considered by Belorizky *et al* [20], i.e. either the 3d–5d or the 5d–4f exchange interactions. Both types of exchange interaction are regarded as distance dependent. When carbon atoms enter interstitially into the lattice, the distance between 4f and 5d electrons changes little, whereas the 3d–5d exchange interaction is reduced owing to the increased distance d_{RT} between R and T atoms.

Inspection of the values of the saturation magnetization σ_s in table 1 shows the ferrimagnetism in the $R_2Fe_{17}C_{1.5}$ and $R_2Fe_{17}C_{2.0}$ series. Expressing $M_s = M_{Fe} - M_R = 17\mu_{Fe} - 2\mu_R$ and using the free-ion values $\mu_R = g_J J\mu_B$ for the R moments, we can obtain the Fe sublattice magnetization M_{Fe} which can be seen in table 1, eighth column. It is interesting to note that the Fe sublattice magnetization in the 2:17 carbides is almost the same, confirming the volume dependence of the Fe–Fe exchange interaction.

For $Er_2Fe_{17}C_{1.5}$ and $Er_2Fe_{17}C_{2.0}$, spin reorientation exists at about $T_{sr} \simeq 133$ K and 141 K, respectively, as shown in figure 6. It is known that the spin reorientation comes from the competition between the different temperature dependences of the rare-earth and Fe sublattice anisotropies. In the 2:17 structure, the second-order Stevens coefficient α_J is expected to have a positive sign for Er [21]; because of the dominant easy-plane Fe sublattice anisotropy, no spin reorientation can be observed for the Er_2Fe_{17} compound. As inferred from figure 1, carbon atoms are located very close to the rare-earth sites and affect fairly markedly the crystalline electric

field experienced by the 4f electrons of the R atoms. When more carbon atoms enter into the lattice, the anisotropy of the Er sublattice increases and a higher spin reorientation temperature appears.

4. Conclusions

(1) The highly stable carbides $R_2Fe_{17}C_x$ ($x = 1.5$, 2.0) with R ≡ Y, Gd, Tb, Dy, Ho, Er were obtained by the melt-spinning method.

(2) The structures of $R_2Fe_{17}C_{1.5}$ and $R_2Fe_{17}C_{2.0}$ are rhombohedral Th_2Zn_{17} type, and the unit-cell volume increase is 4–5%.

(3) The Curie temperature is enhanced enormously because of the increased Fe–Fe exchange interaction, accompanied by the unit-cell volume expansion; the R–Fe interactions are somewhat weakened.

(4) This work implies a possible new way for sintering permanent magnets, such as $Sm_2Fe_{17}C_x$ applications.

Acknowledgment

This work was supported by the National Natural Science Foundation of China.

References

[1] Wang Xian-Zhong, Donnelly K, Coey J M D, Chevalier B, Etourneau J and Berlureau T 1988 *J. Mater. Sci.* **23** 329
[2] Zhong Xia-Ping, Radwanski R J, de Boer F R, Jacobs T H and Buschow K H J 1990 *J. Magn. Magn. Mater.* **86** 333
[3] Coey J M D and Hong Sun 1990 *J. Magn. Magn. Mater.* **87** L251
[4] Hong Sun, Coey J M D, Otani Y and Hurley D P F 1990 *J. Phys.: Condens. Matter* **2** 6465
[5] Buschow K H J, Coehoorn R, de Mooij D B, de Waard K and Jacobs T H 1990 *J. Magn. Magn. Mater.* **92** L35
[6] Coey J M D, Lawer J F, Hong Sun and Allan J E M 1991 *J. Appl. Phys.* **69** 3007
[7] Katter M, Wecker J, Schultz L and Grossinger R 1990 *J. Magn. Magn. Mater.* **92** L14
[8] de Mooij D B and Buschow K H J 1988 *J. Less-Common Met.* **142** 349
[9] Jacobs T H, Dirken M W, Thiel R C, de Jongh L J and Buschow K H J 1990 *J. Magn. Magn. Mater.* **83** 293
[10] Coene W, Hakkens F, Jacobs T H, de Mooij D B and Buschow K H J 1990 *J. Less-Common Met.* **157** 255
[11] Hong Sun, Hu Bo-Ping, Li Hong-Shuo and Coey J M D 1990 *Solid State Commun.* **74** 727
[12] Kou X C, Grossinger R, Jacobs T H and Buschow K H J 1990 *J. Magn. Magn. Mater.* **88** 1
[13] Miraglia S, Soubeyroux J L, Kolbeck C, Isnard O, Fruchart D and Guillot M 1990 *J. Less-Common Met.* **162** 273
[14] Helmholdt R B and Buschow K H J 1989 *J. Less-Common Met.* **155** 15
[15] Coey J M D, Hong Sun, Otani Y and Hurley D P F 1991 *J. Magn. Magn. Mater.* **98** 76
[16] Liao L X, Chen X, Altounian Z and Ryan D H 1992 *Appl. Phys. Lett.* **60** 129
[17] Kuhrt C, Katter M, Wecker J, Schnitzke K and Schultz L 1992 *Appl. Phys. Lett.* **60** 2029
[18] Miedema A R, Niessen A K, de Boer F R, Boom R and Mattens W C M 1988 *Cohesion in Metals* (Amsterdam: North-Holland)
[19] Radwanski R J, de Boer F R, Franse J J M and Buschow K H J 1989 *Physica* B **159** 311
[20] Belorizky E, Fremy M A, Gavigan J P, Givord D and Li H S 1987 *J. Appl. Phys.* **61** 3971
[21] Greedan J E and Rao V U S 1973 *J. Solid State Chem.* **6** 387